



NAVAL POSTGRADUATE SCHOOL

MONTEREY, CALIFORNIA

THESIS

**APPARATUS FOR STUDY OF ION-THRUSTER
PROPELLANT IONIZATION**

by

Frank Harrison Perry, Jr.

December 2006

Thesis Advisor:
Co-Advisor:

Oscar Biblarz
Jose O. Sinibaldi

Approved for public release; distribution is unlimited

THIS PAGE INTENTIONALLY LEFT BLANK

REPORT DOCUMENTATION PAGE			<i>Form Approved OMB No. 0704-0188</i>	
Public reporting burden for this collection of information is estimated to average 1 hour per response, including the time for reviewing instruction, searching existing data sources, gathering and maintaining the data needed, and completing and reviewing the collection of information. Send comments regarding this burden estimate or any other aspect of this collection of information, including suggestions for reducing this burden, to Washington headquarters Services, Directorate for Information Operations and Reports, 1215 Jefferson Davis Highway, Suite 1204, Arlington, VA 22202-4302, and to the Office of Management and Budget, Paperwork Reduction Project (0704-0188) Washington DC 20503.				
1. AGENCY USE ONLY (Leave blank)		2. REPORT DATE December 2006	3. REPORT TYPE AND DATES COVERED Master's Thesis	
4. TITLE AND SUBTITLE Apparatus for Study of Ion-Thruster Propellant Ionization			5. FUNDING NUMBERS	
6. AUTHOR(S) Frank Harrison Perry, Jr.				
7. PERFORMING ORGANIZATION NAME(S) AND ADDRESS(ES) Naval Postgraduate School Monterey, CA 93943-5000			8. PERFORMING ORGANIZATION REPORT NUMBER	
9. SPONSORING /MONITORING AGENCY NAME(S) AND ADDRESS(ES) N/A			10. SPONSORING/MONITORING AGENCY REPORT NUMBER	
11. SUPPLEMENTARY NOTES The views expressed in this thesis are those of the author and do not reflect the official policy or position of the Department of Defense or the U.S. Government.				
12a. DISTRIBUTION / AVAILABILITY STATEMENT Approved for public release; distribution unlimited			12b. DISTRIBUTION CODE A	
13. ABSTRACT (maximum 200 words) <p>Electric propulsion thrusters are considered to be candidates for microsatellites; ion engines are among the most scalable. Miniaturizing the ion engine will require novel concepts for the ionizer. MEMS, nanotechnology and other new technologies are expected to impact here. This thesis explores the use of these technologies to enable a new design for ion-thruster propellant ionization. An ideal approach, using expensive fabrication processes, is first described. This approach could prove to be a good method for testing and for the collection of precise data.</p> <p>A cost effective approach, on which our testing is based, is then discussed in detailed. After assembling a facility which uses existing vacuum systems and available instrumentation, we manufactured and tested miniature discharge geometries consisting of commercial 2"x2" copper-clad wafers. Three nominal insulator thickness' were used, 0.005," 0.010" and 0.115." The wafers were each drilled with 9 equal wholes of diameters 300, 400, and 500 µm. A total of 12 wafers were tested (including 3 widths without wholes for a baseline) for the breakdown voltage as a function of argon pressure in the range of 10 to 1000 mTorr. Results indicate that argon breakdown may occur in the holes consistent with the classical Paschen curves.</p>				
14. SUBJECT TERMS Ion Propulsion, Ion Engine, MSE array, Paschen Curve, Ionizer			15. NUMBER OF PAGES 71	
			16. PRICE CODE	
17. SECURITY CLASSIFICATION OF REPORT Unclassified	18. SECURITY CLASSIFICATION OF THIS PAGE Unclassified	19. SECURITY CLASSIFICATION OF ABSTRACT Unclassified	20. LIMITATION OF ABSTRACT UL	

THIS PAGE INTENTIONALLY LEFT BLANK

Approved for public release; distribution is unlimited

APPARATUS FOR STUDY OF ION-THRUSTER PROPELLANT IONIZATION

Frank Harrison Perry, Jr.
Lieutenant, United States Navy
B.S. in History, United States Naval Academy, 1997

Submitted in partial fulfillment of the
requirements for the degree of

MASTER OF SCIENCE IN ASTRONAUTICAL ENGINEERING

from the

**NAVAL POSTGRADUATE SCHOOL
December 2006**

Author: Frank Harrison Perry, Jr.

Approved by: Oscar Biblarz
Thesis Advisor

Jose O. Sinibaldi
Co-Advisor

Anthony J. Healey
Chairman, Department of Mechanical and
Astronautical Engineering

THIS PAGE INTENTIONALLY LEFT BLANK

ABSTRACT

Electric propulsion thrusters are considered to be candidates for microsatellites; ion engines are among the most scalable. Miniaturizing the ion engine will require novel concepts for the ionizer. MEMS, nanotechnology and other new technologies are expected to impact here. This thesis explores the use of these technologies to enable a new design for ion-thruster propellant ionization. An ideal approach, using expensive fabrication processes, is first described. This approach could prove to be a good method for testing and for the collection of precise data.

A cost effective approach, on which our testing is based, is then discussed in detailed. After assembling a facility which uses existing vacuum systems and available instrumentation, we manufactured and tested miniature discharge geometries consisting of commercial 2"x2" copper-clad wafers. Three nominal insulator thickness' were used, 0.005," 0.010" and 0.115." The wafers were each drilled with 9 equal wholes of diameters 300, 400, and 500 μm . A total of 12 wafers were tested (including 3 widths without wholes for a baseline) for the breakdown voltage as a function of argon pressure in the range of 10 to 1000 mTorr. Results indicate that argon breakdown may occur in the holes consistent with the classical Paschen curves.

THIS PAGE INTENTIONALLY LEFT BLANK

TABLE OF CONTENTS

I.	INTRODUCTION.....	1
II.	ION ENGINE OPERATION AND PROBLEM DEFINITION.....	3
	A. ION THRUSTER OPERATION.....	4
III.	TECHNICAL APPROACH.....	7
	A. BACKGROUND	7
	B. EXPERIMENTAL PROCEDURES	12
IV.	MANUFACTURING ASPECTS.....	19
	A. FUTURE MANUFACTURING	19
	B. ELEMENTS OF MANUFACTURING	20
	1. Ideal Wafers	20
	2. Actual Wafers.....	25
	C. EQUIPMENT DESCRIPTION	26
V.	CONCLUSIONS AND RECOMMENDATIONS.....	37
	A. SUMMARY	37
	B. RECOMMENDATIONS FOR FUTURE WORK.....	37
	APPENDIX A. GLOSSARY OF TERMINOLOGY	39
	APPENDIX B. MATLAB CODE FOR GRAPHS	41
	APPENDIX C. GRAPHS OF SAMPLES BY HOLE SIZE.....	45
	APPENDIX D. VACUUM SET-UP DIAGRAMS	47
	A. THIS SECTION WILL COVER THE PROCEDURE FOR VACUUM CHAMBER OPERATION	47
	B. THIS SECTION WILL COVER THE PROCEDURE FOR INSTRUMENT PANEL OPERATION.....	50
	LIST OF REFERENCES	53
	INITIAL DISTRIBUTION LIST	55

THIS PAGE INTENTIONALLY LEFT BLANK

LIST OF FIGURES

Figure 1.	Ion Engine Test	2
Figure 2.	Ion Thruster Operation.....	4
Figure 3.	Microstructure being used in Ionization Process	8
Figure 4.	Pressure*Distance vs. Breakdown Voltage	9
Figure 5.	Second Graph of Pressure*Distance vs. Breakdown Voltage	9
Figure 6.	Dimensionless Paschen Curve	11
Figure 7.	Copper-glass copper composite microstructure with 3x3 matrix of holes	12
Figure 8.	Schematic of Vacuum Set-up.....	13
Figure 9.	Electrical Rack	14
Figure 10.	Sample wafer attached with plastic clamps	15
Figure 11.	Glow discharge of sample after achieving breakdown voltage	16
Figure 12.	Step diagram showing etching of SiO_2 wafer	19
Figure 13.	Diagram of the Sputtering Process	23
Figure 14.	A spinner used to apply photo resist to the surface of a silicon wafer.....	24
Figure 15.	Electroplating process: For this diagram the anode is a silver bar and the cathode is an iron spoon.....	25
Figure 16.	300 μm sample diameter hole in $Cu - Si_2O_3 - Cu$ structure (Microscope Facility-courtesy of Prof. McNelley).....	26
Figure 17.	400 μm sample diameter hole in $Cu - Si_2O_3 - Cu$ structure (Microscope Facility-courtesy of Prof. McNelley).....	27
Figure 18.	500 μm sample diameter hole in $Cu - Si_2O_3 - Cu$ structure (Microscope Facility-courtesy of Prof. McNelley).....	27
Figure 19.	Kepeco Labs 500R-B Power Supply Voltage	29
Figure 20.	Terranova Model 505A Digital Pressure Recorder	29
Figure 21.	Varian 880RS Vacuum Ionization Gauge.....	30
Figure 22.	The voltmeter (left) and amp meter (right) used for the experiments.....	30
Figure 23.	Jason Cooper recording the breakdown voltage on a sample	31
Figure 24.	A close-up of the breakdown voltage occurring on the Tektronix TDS 1012.....	31
Figure 25.	System set-up displaying the Varian Turbo-V1000.....	32
Figure 26.	Varian SD-450 (left) and Edwards roughing pump (right).....	33
Figure 27.	Precise metering value	34
Figure 28.	Argon bottles next to vacuum chamber set-up	34
Figure 29.	Precision Drill Press used to create the micron holes	35
Figure 30.	Optical Microscope used to measure the MSE	35
Figure 31.	Etching tank	36
Figure 32.	Experimental Results (Paschen Curves) (300 μm).....	45
Figure 33.	Experimental Results (Paschen Curves) (400 μm).....	45
Figure 34.	Experimental Results (Paschen Curves) (500 μm).....	46
Figure 35.	Schematic drawing of vacuum set-up	48

Figure 36.	Schematic drawing of Varian 880RS Vacuum Ionization Gauge	49
Figure 37.	Schematic of Argon bottle, gauge, and values used for metering	49
Figure 38.	Schematic drawing of Electrical Rack.....	51

LIST OF TABLES

Table 1.	Chart of various thicknesses of samples used.....	28
----------	---	----

THIS PAGE INTENTIONALLY LEFT BLANK

ACKNOWLEDGMENTS

First and foremost, I would like to give thanks to God. Without the almighty none of this would be possible. My parents Mr. and Mrs. Frank and Delores Perry have been lifelong motivators. They provided me with the support and confidence to successfully complete this program and my thesis research. Jason Cooper my micro-ION Engine collaborator was also a motivating factor in helping me get through this challenging masters program and thesis research. We helped each other when times got hard and I thank him for his steadfast friendship. Prof. Biblarz and Prof. Sinibaldi were both instrumental in aiding me to better understand the subject material and with keeping me on a strict timeline. They were always available to answer questions keeping an open door policy at all times. I would also like to acknowledge a few NPS technical staff who worked very hard to make sure that my apparatus was connected and set-up correctly abiding by all safety regulations. When items broke or stopped working, they were there to help in anyway they could. Without Mr. George Jaksha, Mr. Sam Barone, and Mr. Don Snyder my thesis could not have been completed on time and all data recorded would not have been possible. Dr. Leonard Ferrari for approving the initial \$5,000 research funds to initiate this research effort; and finally Dr. Gamani Karunasiri for providing the bell-jar and vacuum system.

THIS PAGE INTENTIONALLY LEFT BLANK

I. INTRODUCTION

Ion propulsion is an engine technology that involves the ionization of gas to propel a spacecraft. Gases such as Xenon or Argon are ionized and electrically propelled to very high speeds to produce thrust. Ion engines can deliver a small thrust at high specific impulses which is of interest for space applications. Figure 1 below shows an ion engine which flew in NASA's Deep Space 1 mission. The National Aeronautics and Space Administration (NASA) developed its first ion engine at Glenn Space Center in 1960.

As of now, only the Hall thruster and the FEEP (field emission electric propulsion) engine are being considered as viable candidates for micropropulsion. This work should shed more light on the potential of the ion engine for micropropulsion. It should also help with present applications of electric propulsion.

This work helps describe how to use MEMS (Microelectromechanical Systems) fabrication processes to develop a micropropulsion ion engine. These engines have advantages over current Ion Engines such as: much lower voltage requirements, elimination of large (and heavy) magnets in the ionization chamber, substantial reduction in power units, increased payload mass fraction, etc. The theory behind this process was examined in some detail for further understanding. Specifically, we seek to understand and improve upon Penache's work. Her work described how microtechnology enabled the development of micro-ionization structures. The work herein extends her work and applies it to the Ion Engine. An example of such an Ion Engine (see Figure 1) is shown below.

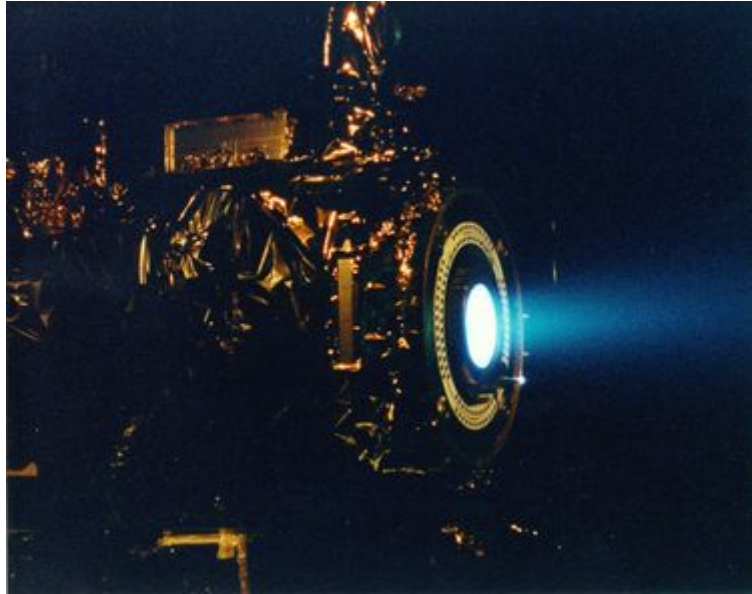


Figure 1. Ion Engine Test¹

¹ Wikipedia, http://en.wikipedia.org/wiki/Ion_engines (December 2006).

II. ION ENGINE OPERATION AND PROBLEM DEFINITION

Modern ion thrusters use inert gases such as Argon or Xenon for propellant as compared to Cesium or other non-inert gases. The majority of these thrusters use Xenon, which is chemically inert. It has a large MW which enables a higher delta mv. In present day ion thrusters, electrons are created via hollow cathodes, called the discharge cathode, located at the center of the engine on the upstream end². The electrons flow out of the discharge cathode and are attracted to the discharge chamber walls, which are charged to a positive potential by the thruster's power supply.

The electrons from the discharge cathode ionize the propellant by means of electron bombardment. Magnets are placed along the discharge chamber walls so that as electrons approach the walls, they spiral in the discharge chamber, thus maximizing the length of time that electrons interact with the propellant. This process optimizes the chance of ionization which makes the ionization process reach peak efficiency.

In an ion thruster, positive ions are accelerated by electrostatic forces. The electric fields used for acceleration are generated by electrodes (in a grid- or screen-like configuration) are positioned at the downstream end of the ionizer. Each set of electrodes, called grids, contain thousands of coaxial apertures. Each set of apertures acts as a lens that electrically focuses ions through the optics. Most ion thrusters use a two-electrode system, where the upstream electrode is positively charged, and the downstream electrode has a highly negative charge. Since the ions are generated in a region of high positive and the accelerator grids' potential is negative, the ions are attracted toward the accelerator grid and are then focused out of the discharge chamber through the apertures, creating thousands of minute ion jets. The stream of all the ion jets together is called the ion beam (see Figure 2). The thrust force is the product of the mass flow rate and the exhaust velocities. The exhaust velocity of the ions in the beam is based on the voltage applied to the optics. While a chemical rocket's top speed is limited by the thermal

² Boeing, <http://www.boeing.com/defense-space/space/bss/factsheets/xips/nstar/ionengine.html>. (December 2006).

capability of the rocket nozzle, the ion thruster's top speed is limited by the voltage that can be applied to the ion optics, which is only limited by the vacuum breakdown. The high specific impulse can be varied by varying the accelerator voltage.

Because the ion thruster ejects positive ions, an equal amount of negative charge must be expelled to keep the total charge of the exhaust beam neutral. A second hollow cathode called the neutralizer is located on the downstream perimeter of the thruster and expels the needed electrons.

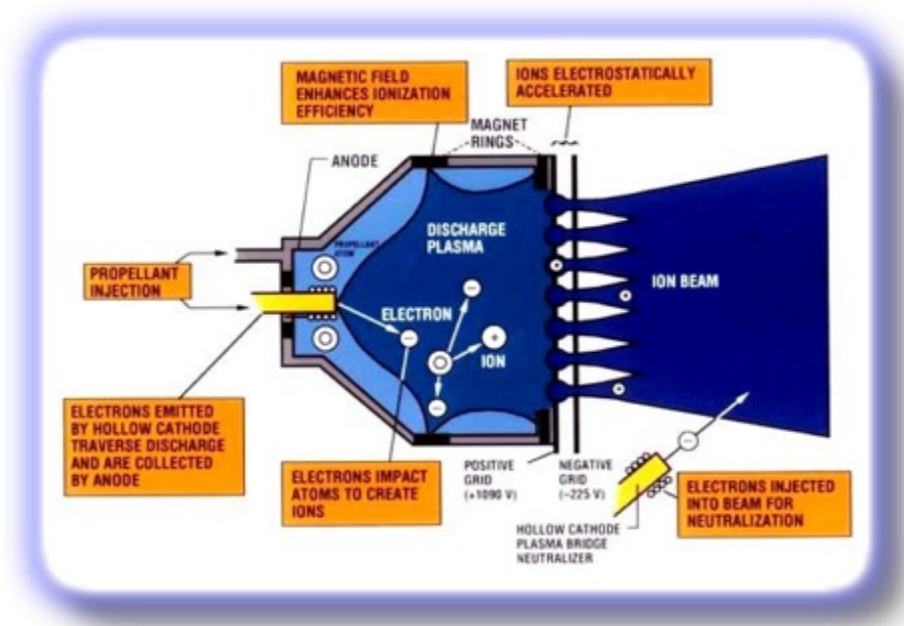


Figure 2. Ion Thruster Operation³

A. ION THRUSTER OPERATION

The ion propulsion system consists of five main parts: the power source, power processing unit, propellant management system, the control computer, and the ion thruster. The ion propulsion system power source can be any source of electrical power, but solar and nuclear are the primary options. A solar-electric propulsion system uses sunlight and solar cells for power generation. A nuclear-electric propulsion system uses a nuclear heat source coupled to an electric generator. The power processing unit converts

³ Wikipedia, http://en.wikipedia.org/wiki/Image:DS1_Ion_Engine_Diagram.jpg (December 2006).

the electrical power generated by the power source into the power required for each component of the ion thruster. It generates the voltages required by the ion optics and discharge chamber and the high currents required for the hollow cathodes. The propellant management system controls the propellant flow from the propellant tank to the thruster and hollow cathodes.

Modern propellant management systems have evolved to a level of sophisticated design that no longer requires moving parts. “The control computer controls and monitors system performance. The ion thruster then processes the propellant and power to perform work. Modern ion thrusters are capable of propelling a spacecraft up to 90,000 meters per second (about 200,000 miles per hour). To put that into perspective, the space shuttle is capable of a top speed of around 18,000 mph. The tradeoff for this high top speed is low thrust (or low acceleration). Thrust is the force that the thruster applies to the spacecraft.”⁴ To compensate for low thrust, the ion thruster must be operated for a long time for the spacecraft to reach its top speed. Ion thrusters use inert gas for propellant, eliminating the risk of explosions associated with chemical propulsion. The usual propellant is Xenon, but other gases such as Krypton and Argon may be used also. Using Argon is proposed herein due to its low cost and abundance. Yet, there is still the need to show an ion engine capable of producing acceptable performance on gases such as Argon⁵.

The ion engine is a complex machine that requires a deeper look into the ionization process on an atomic level in order to understand. This will also aid in understanding why certain materials were chosen in order to maximize the ionization process, which ultimately produces thrust for the ion engine. Ionization is the process of breaking electrons free from the outermost or valence shell of atoms and the most in need of improvement in such thrusters.

⁴ John Glenn Research Center, National Aeronautics and Space Administration, <http://www.grc.nasa.gov/WWW/ion/overview/overview.htm>. (December 2006).

⁵ E. Nasser, *Fundamentals of Gaseous Ionization and Plasma Electronics*, John Wiley & Sons, Inc., 1971.

THIS PAGE INTENTIONALLY LEFT BLANK

III. TECHNICAL APPROACH

A. BACKGROUND

In order to produce the ionic thrust needed to propel a spacecraft into deep space, a requirement exists for cathodes from which electrons can be easily extracted. Releasing these electrons can be done in several ways. Thermionic photo emission and field emissions are valid options. All the properties of the plasma ionization process are not well known and may not fit into the idea of a miniature propulsion source, which the micro ionizer proposed herein seeks to provide. Copper was used in its intrinsic state as an electrode material for our design.

With this basic knowledge in hand, a microstructure based cathode was designed in L-Edit. L-Edit is a computer aided VLSI design tool program which allows you to perform micromachine designs, and circuit board layouts. It allows you to displays multi-layer machines using various materials can colors. Finally, you can simulate real animation of your micromachine in the SPICE program. For our experiments, we chose electron bombardment as the method for propellant ionization.



The ionization process involved in this microstructure ionizer are very similar to the fluorescent lights found in most homes in which electrons flow from the negative side to the positive side creating a glow initiated by a breakdown voltage which we will discuss later. The microstructure consists of two Copper plates “electrodes” with a glass insulator between them and though holes in a matrix (3 x 3 in this case) are placed in the middle. These holes are required to ionize the gas while allowing flow through the proposed micro-ionizer, thus removing electrons and leaving positive ions that are feed into the accelerator for propulsion. When a sufficient voltage is applied across these copper layers, a strong electric field is generated capable of causing breakdown of the gas and thus allowing current to pass through the ionized gas after breakdown.

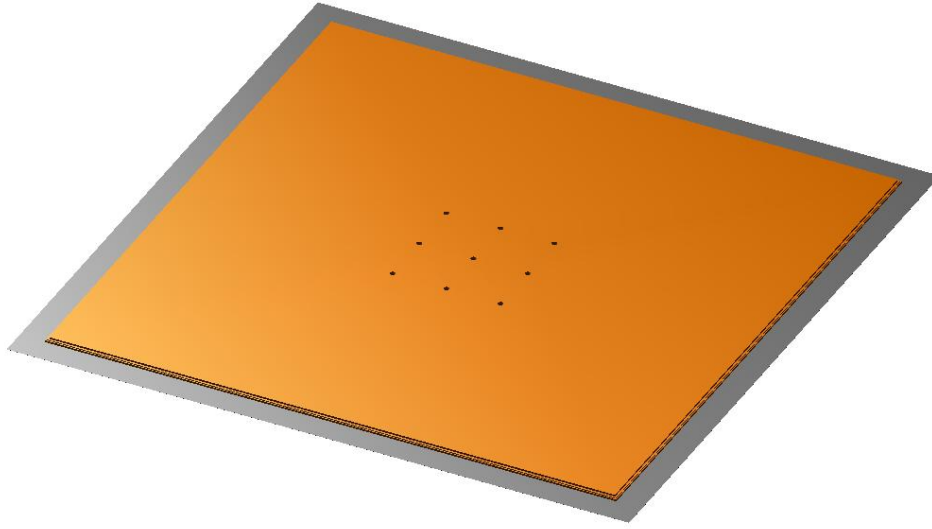


Figure 3. Microstructure being used in Ionization Process⁶

As stated earlier, this micro-ionizer arrangement has a series of through holes going through it which allows the gas to flow through. Each hole is a source of microdischarge that takes place between the two copper electrodes (see Figure 3). The field is capable of reaching strengths near 10^6 V/cm ⁷. The distance between the copper electrodes needs to be as small as $100 \mu\text{m}$ in order to allow high pressure operation. Our immediate objective is to generate the Paschen curves, using various configurations in which the thickness of the dielectric layer is changed, the diameter of the holes is changed, the thickness of the copper layers is also changed as well as the operating pressures and voltages. The Paschen curve is a plot of the breakdown voltage vs. pd (pressure times electrode separation distance). Figures 4 below show this. Earlier experiments have found that as pd is increased the voltage needed to create ions in a discharge goes through a minimum. This is the reason that the thickness of the insulator

⁶ L-Edit Design Tool.

⁷ M. C. Penache, "Study of High Pressure Glow Discharges Generated by MicroStructured Electrode (MSE) Arrays," PhD Dissertation, Frankfurt am Main University, Germany, 2002.

(glass in our case) is varied to change the distance between two discharge plates at a given gas pressure. Then pressure is changed during each wafer experiment.

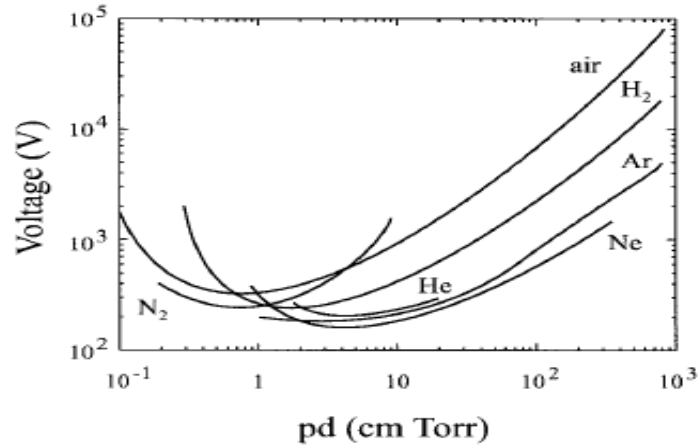


Figure 4. Pressure*Distance vs. Breakdown Voltage⁸

If the distance between electrodes is fixed, and the pressure is decreased, the breakdown voltage first decreases reaching a minimum and, then increases exponentially. Figure 4 depicts this process for various gases. The minimum point of the breakdown voltage is the region where the ionization of the electrons is most efficient.

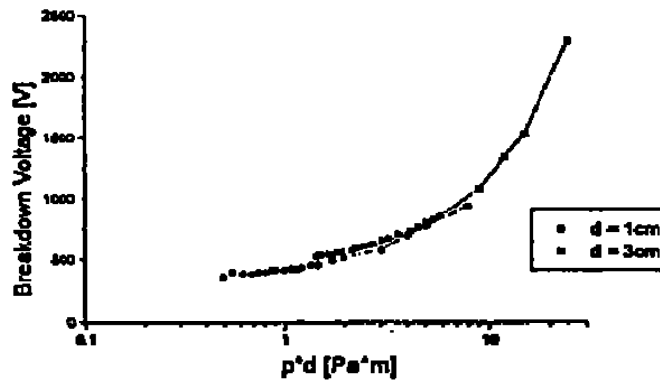


Figure 5. Second Graph of Pressure*Distance vs. Breakdown Voltage⁹

⁸ Google,
<http://images.google.com/images?svnum=10&hl=en&lr=&q=paschen+curves&btnG=Search>. (December 2006).

⁹ Google,
<http://images.google.com/images?svnum=10&hl=en&lr=&q=paschen+curves&btnG=Search>. (December 2006).

For the current experiments, the least amount of voltage necessary to produce a current (i.e. the breakdown voltage) is of most importance. The theory for Paschen curves for parallel plates is used to compare the experimental results in Cooper's work [Jason Cooper-Thesis Research, "Study of a Novel Ionization Chamber for Ion Thrusters"-Naval Postgraduate School thesis-December 2006]. Therefore it shall be introduced here. The Paschen curve equation for parallel plates is:

$$V_B = \frac{B \cdot pd}{\ln(pd) + \ln(A/l(\ln + \gamma^{-1}))} \quad (2)$$

The pd is the product of pressure and distance, γ is the cathode-surface secondary emission coefficient, and A and B are experimentally determined constants for a given gas (which can be either Argon or Xeon for our experiments). Keeping the voltage constant yields a constant electric field in a given electrode configuration. Here "d" is the thickness of the dielectric layer between the copper electrodes.

The Paschen curve equations can be written down further in a dimensionless for (See Figure 6):

$$Y = \frac{X}{\ln(X)} \quad \text{where} \quad Y = \left(\frac{A}{\ln(1 + r^{-1})} \right) \frac{V_d}{B} \quad X = \left(\frac{A}{\ln(1 + r^{-1})} \right) pd \quad (3)$$

We now have the equation:

$$Y = X/\ln(X) \quad (4)$$

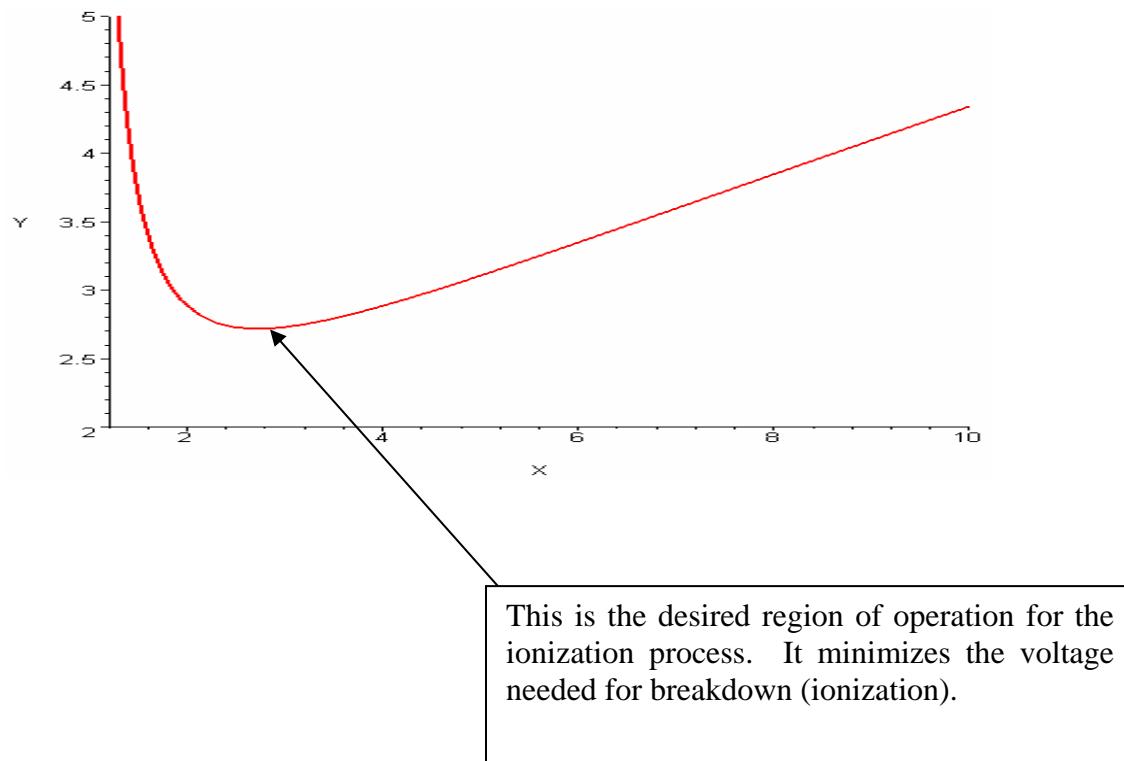


Figure 6. Dimensionless Paschen Curve

Because our electrode geometry is different from the conventional Paschen Law, we have to evaluate two constants experimentally for the following equation:

$$V_B = \left(\frac{C_1(pd)}{\ln[C_2(pd)]} \right) \quad (5)$$

In order to do this, a method had to be developed to obtain the breakdown voltages for each of the test cases and then graph and evaluate the results.

Before beginning the experiments, methods had to be developed to find a way to achieve the following objectives:

- (1) How to measure and backfill Argon to 1 Torr,
- (2) How to throttle the Argon pressure .001-1 Torr
- (3) How to obtain a variable DC voltage 0-400 V
- (4) How to measure voltage and current at the “breakdown” region

- (5) How to mount our samples without short circuiting them
- (6) How to obtain a baseline “breakdown voltage” of the microstructures without holes at a range of pressures up to 1 Torr
- (7) How to cut the 2”x 2” composite structures and create the microstructured holes

The samples included three different thicknesses of 2”x 2” copper-glass-copper composite microstructures with a 3x3 matrix of through holes in the center of each sample (see Figure 7). These holes have diameters of 300, 400, and 500 micrometers and were created using conventional precision machining techniques.

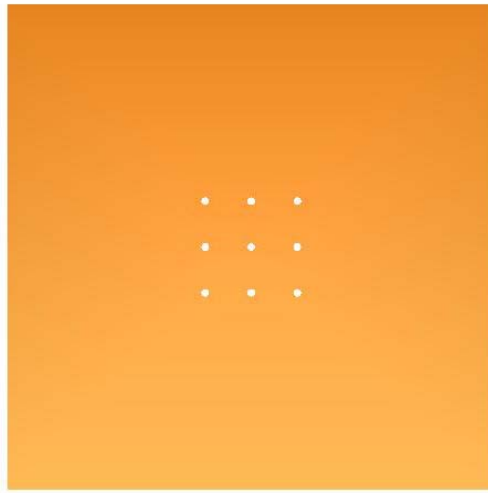


Figure 7. Copper-glass copper composite microstructure with 3x3 matrix of holes¹⁰

B. EXPERIMENTAL PROCEDURES

The setup includes a vacuum chamber, two roughing vacuum pumps, one turbo-molecular vacuum pump, and an electrical rack with instruments (see Figure 9) to measure the voltage and amperage of the samples and to aid in measuring the breakdown voltage. The vacuum chamber simply houses the area where the gas is ionized. It was maintained at a very high vacuum for our experiments. The two roughing pumps were used to reduce the workload on the turbo-molecular vacuum pump when bring the chamber down from very high vacuums. The turbo-molecular vacuum pump was used to decrease the vacuum in the chamber after a very low pressure as achieved. It was the workhorse of our experiments. Finally, the electrical rack housed the voltmeter, amp

¹⁰ L-Edit Design Tool.

meter, and the power source. These were used to provide various power requirements as well as displaying the voltage and current during the experiments. The two roughing pumps aided in getting the vacuum down to the starting vacuum pressure prior to the initiation of the turbomolecular vacuum pump.

There were three available means of measuring the vacuum pressure in and around the chamber via thermal couples (TC) as seen in Figure 8. The three pressure measurement locations on the setup included (TC1, TC2, and TC3). The TC3 position is located just above the shutoff valve in the vacuum chamber. This is measured by the digital pressure recorder which was only capable of measuring a pressure as low as 0.4 millitorr. In order to obtain measurements below this value, the readings of the turbomolecular pump was used. The TC2 position measures the pressure just below the cutoff value and TC1 measures the pressure between the roughing pumps and the turbomolecular pump. These TC measurement positions were all very important during the experiments.

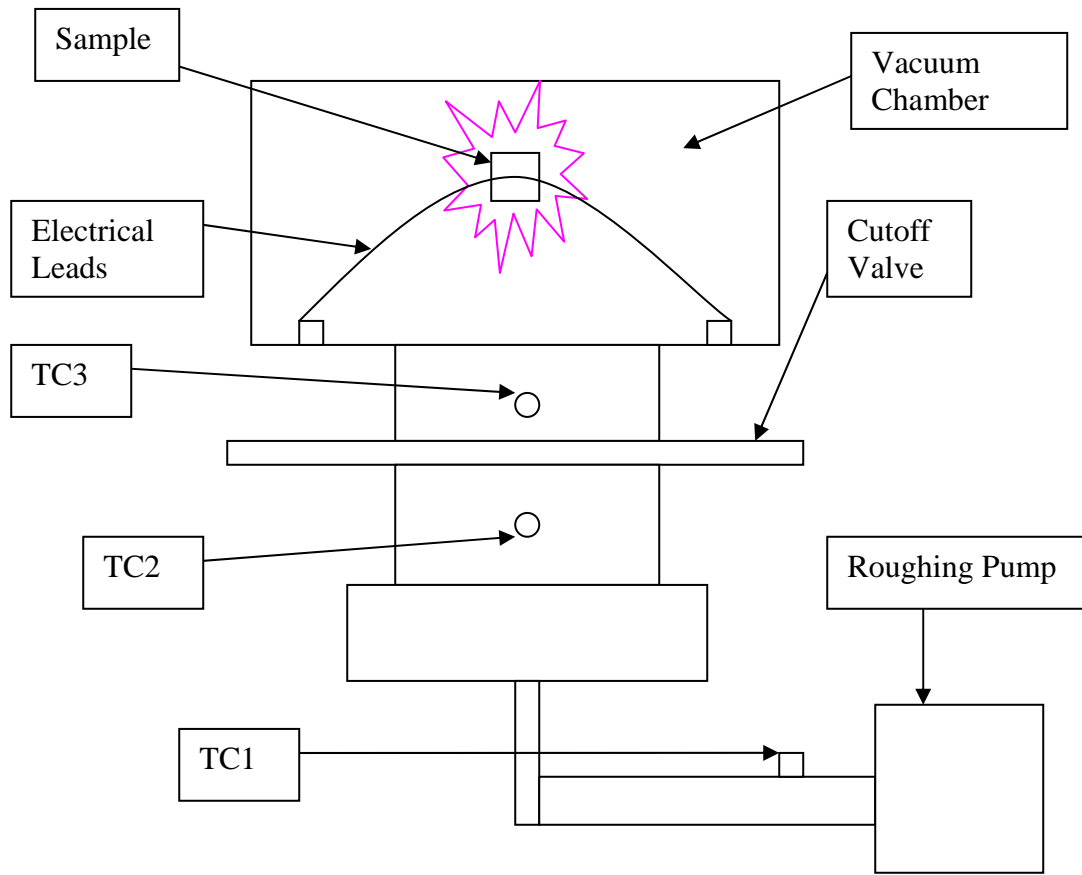


Figure 8. Schematic of Vacuum Set-up

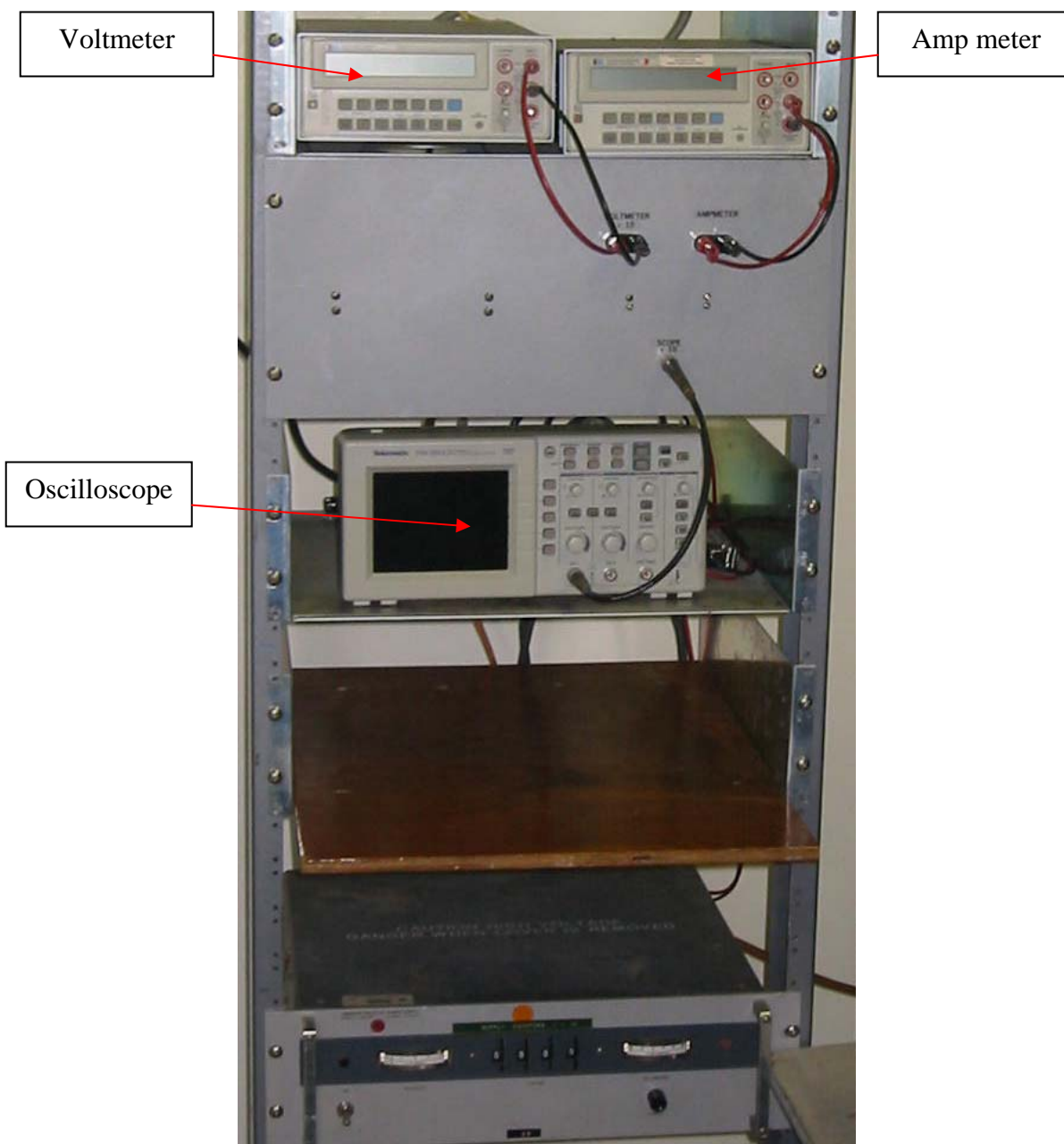


Figure 9. Electrical Rack

The procedure for attaining the breakdown voltage for each sample is very similar. First, the sample is placed into a plastic container of rubbing alcohol solution to remove all contaminants. Then the sample is placed into the chamber attaching it to two copper wires with plastic clamps making sure to attach the wires on opposite sides of the sample to prevent a short circuit (see Figure 10).

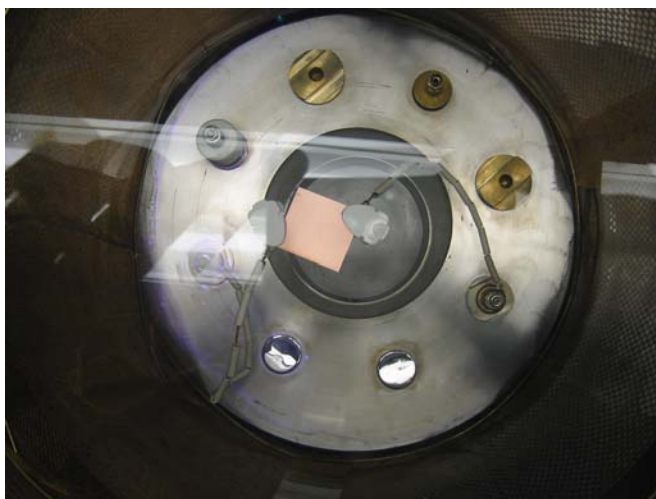


Figure 10. Sample wafer attached with plastic clamps

The lid is then placed over the chamber and the roughing pump is turned on. The roughing pump was usually long enough to achieve the lowest possible pressure. The cutoff value is also kept open in order to achieve this sense the roughing pump was located below the cutoff valve. All measurement positions (TC3, TC2, and TC1) are used. The readings on TC2 and TC1 are used because the TC1 could only read down to 0.4 millitorr and no lower.

To begin the experiments the pumps lowest recorded vacuum was $3.7 \times 10^{-7} \text{ Torr}$. Once this number is achieved, the experiments were ready to commence. Next, the cutoff valve is placed in the closed position and so began the process of backfilling the chamber with Argon. The measurements were taken on each sample at 10 millitorr, 100 millitorr, 1 torr, and then at 10 millitorr again. The gauge measuring at the TC3 position is very sensitive at 10 millitorr. Therefore, at very low pressures, the pressure keeps climbing. This was the result of a small leak in the system. Once the operating pressure was reached and the vacuum chamber was backfilled with Argon to the target pressure of 10 millitorr, the voltage was ramped up on the sample in 10 Volt increments to obtain the voltage in which breakdown voltage was achieved. The limit of the available high voltage DC power supply was 400 Volts thus no tests were performed above 400V. The TC2 measurement position was less sensitive at 75 millitorr and lower. This process was

repeated continuously by ramping up the voltage up to find the next breakdown voltage at the new target pressure. See Figure 11 shows the plasma appearance during breakdown.



Figure 11. Glow discharge of sample after achieving breakdown voltage

Because many different measurements were taken on each sample along with the need to achieve such a low beginning pressure which took several hours to achieve, experimentation was limited to performing experiments on a maximum of 2 samples per day. The data was evaluated after performing the experiments on the 300, 400, and 500 micrometer samples for all three thicknesses.

Initially, the data did not produce a Paschen curve. The data were very sporadic to say the least. From a manufacturing and design standpoint, the vacuum chamber set up was flawed. It was determined that due to the glow discharge happening all around the chamber, the breakdown was not being concentrated around the holes as they should be. The current was finding a way to ground other than across the Copper electrodes; therefore giving faulty data. To remedy this, two insulating plastic cups were placed over

the nodes that were hooked up to the current producing device. This provided a non-conducting material barrier thereby limiting the current flow to other areas to achieve grounding.

Furthermore, it was discovered that all vacuum pumps required electrical isolation from the vacuum chamber to cure ground loops that were detected.

After all of these modifications, the breakdown was now clearly happening at the holes in the center of the samples. By varying the pressures at which the breakdown voltages were recorded, the Paschen curves were generated was achieved for each of the samples at all thicknesses. As a result of the changes all new data had to be taken for all the samples again.

THIS PAGE INTENTIONALLY LEFT BLANK

IV. MANUFACTURING ASPECTS

A. FUTURE MANUFACTURING

One of the goals for this work has been to miniaturize the ionizer part of the Ion Engine. This can be performed by incorporating MEMS (Microelectromechanical Systems) technology. Currently, the most appropriate manufacturing technique for production levels has been identified-surface and bulk micromachining on wafers (see Figure 12). To do this it is necessary to select the appropriate materials for the wafer substrate. The wafer consists of a three layer composite with perhaps the top layer and the bottom layer of silicon carbide (SiC) and an insulating layer of perhaps silicon dioxide (SiO_2), sandwiched between (see Figure 12).

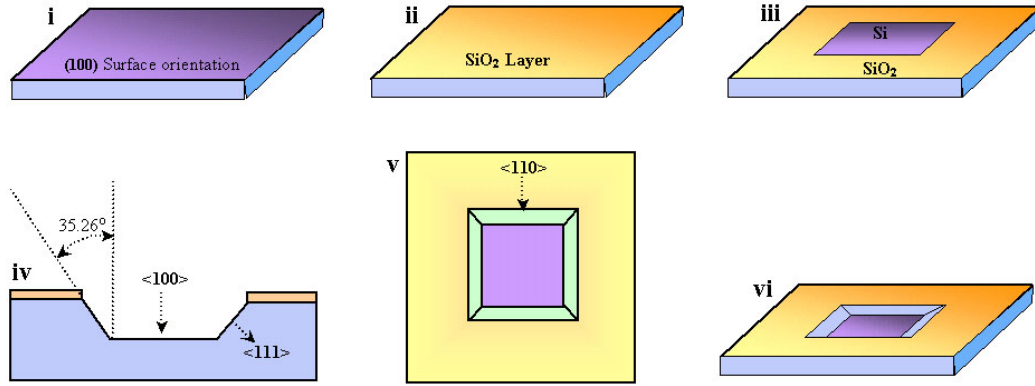


Figure 12. Step diagram showing etching of SiO_2 wafer¹¹

Other material options can be investigated for ease of fabrication and for cost considerations. Once the wafer composite is selected a software tool such as L-Edit long with MEMS Exchange can be utilized to formulate a process whereby micrometer scale holes are etched through with nanometer scale resolution. Also important, once the

¹¹ Parallel Synthesis Technologies Inc., www.parallel-synthesis.com/SiliconMicrofabrication.htm. (December 2006).

fabrication is done, would be to return the microstructure for carbon nanotube emplacement whereby a layer of carbon nanotubes would be grown along the cathode walls of each of the holes.¹².

It is hoped that such a system would be able to help with the necessary ionization of an inert gas like Argon or Xenon once a voltage difference is applied across the top and bottom layers. The carbon nanotubes would generate an electric field strong enough to produce copious electrons by field emission. The gas as it passes through the holes in the wafer composite would be ionized at lower voltages. Once the gas is ionized the ions are electrostatic accelerated by the use of an accelerator grid which is negatively charged. Ions exit the accelerator as an ion beam, which is then neutralized.

B. ELEMENTS OF MANUFACTURING

1. Ideal Wafers

To create a three-dimensional microstructure, the L-edit was used. Currently, the process of researching the idea of using the MEMS Exchange to aid us in designing our microstructure is being entertained.

In order to have wafers manufactured (outside the virtual environment) in real life, a fabrication process that currently exists needed to be used. However, L-Edit will allow the design of items that are not capable of being designed in the real world. The design at hand consists of a matrix of holes perforated in a composite sheet made out of two conducting layers of SiC separated by an insulator. Each hole needs to be a source of micro discharge between the two conducting layers representing the electrodes. Different materials could be used for the dielectric spacer such as glass, polyimide, or ceramic with a thickness of 50-250 micrometers. Glass may be used because it makes a great insulator and is cheap to manufacture. A spacing of 50 micrometers is a parameter estimated to obtain maximum efficiency out of the ion engine. Although our electrodes are made of copper, it was envisioned that SiC layers of around 100 micrometers thick will be used as the conducting layers due to their tough material properties that allow for continuous ion bombardment with minimal degradation. The holes have been designed to have nominal diameters of 70 micrometers. Circles are chosen although the initial etching can make squares. Previous studies of the ion engine thrust production tells us that there is no

¹² PH3280-MEMS Design I Class.

significant effect on the discharge operation as long as the hole opening is in the range of 70-300 micrometers. The spacing between the holes is 3 mm in order to enable the observation of individual discharges and to reduce the thermal stress on the microstructure¹³.

To create this device in L-edit, a unit cell was specifically created, arrayed, and instanced. Next, the array parameter, which is an elementary operation in L-edit, was set. Then a set for the materials in 3D tools where the material data base is located was created. A process description process step was set and the thickness was entered for the material. The hole size was created by editing the unit cell. Cell-0 was used to create the square. The two conducting layers of copper were deposited to make a hole of radius 70 micrometers. Then placed another layer and etched a square hole again and then another layer and etched a final time. The circle was then placed on the hole layer in edit process definition where the last step was to etch the hole. In short, after each etching event for each surface, the holes were made to get the circle down to the substrate¹⁴.

As stated earlier, the MEMS Exchange aided us in determining a fabrication process. The following question had to be answered. "How do we design a process sequence so that the device we imagine can actually be built?" The process was obtained by contacting the MEMS Exchange fabrication company located in Reston, VA. They plan to use 8 steps for the fabrication of our microstructure. They are:

- 1) Pattern Generation
- 2) Sputter
- 3) Sputter
- 4) Lithography
- 5) Lithography
- 6) Electroplating

¹³ M. C. Penache, "*Study of High Pressure Glow Discharges Generated by Micro-Structured Electrode (MSE) Arrays*," PhD Dissertation, Frankfurt am Main University, Germany, 2002.

¹⁴ M. C. Penache, "*Study of High Pressure Glow Discharges Generated by Micro-Structured Electrode (MSE) Arrays*," PhD Dissertation, Frankfurt am Main University, Germany, 2002.

- 7) Strip
- 8) Miscellaneous

The pattern generation is simply the development of a process to design the microstructure. It is a game plan for developing the structure. The basic wafer description is (for example):

- Number of wafers: 5
- Material: Fused Silica
- Thickness: $250\mu m$
- Diameter: 100mm
- Initial state: virgin
- Surface finish: double side polish

Sputtering is a process whereby atoms in a material are ejected into the gas phase due to the bombardment of the material by energetic ions. It is used for thin-film deposition. Sputtering is largely driven by momentum exchange between the ions and atoms in the material, due to collisions. The process can be thought of as a game of pool, in which the ions are striking a large cluster of atoms (see Figure 13). Although the first collision pushes atoms deeper into the cluster, collisions between the atoms can result in some of the atoms near the surface being ejected away from the cluster. The number of atoms ejected from the surface per ion is called the sputter yield. This is an important measure of the efficiency of the sputtering process. The ions for the sputtering process are supplied by plasma that is induced in the sputtering equipment. Below is a diagram showing the Sputtering process¹⁵. The specifics on the sputtering materials are (for example):

- Material: Gold
- Thickness: $0.2\mu m$
- Critical dimension tolerance: 0.5mm

¹⁵ Sputtering.com, <http://www.sputtering.info/>.(November 2006).

-Mask Coating: Chromium

-Mask material: soda lime 20° C

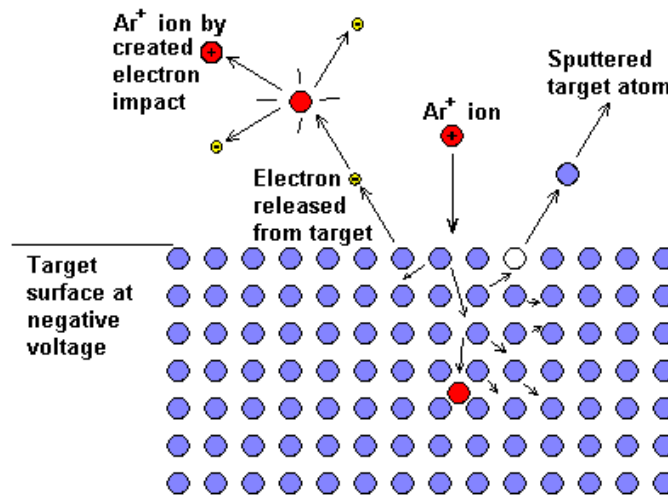


Figure 13. Diagram of the Sputtering Process¹⁶

Lithography is a process used in microstructure fabrication to transfer a pattern from a photo mask to the surface of a substrate. In our case, this will be a series of hole pattern arrays to allow the gas to flow through. Often crystalline silicon in the form of a wafer is used as a choice of substrate, but we will be using glass. A typical lithography procedure would begin by depositing a layer of conductive metal several nanometers thick on the substrate. A layer of photo resist (this is a chemical that hardens when exposed to light) is applied on top of the metal layer. The photo resist is then made very hard by illuminating it. For this purpose a transparent plate with patterns printed on it, called a photo mask, is used together with an illumination source to shine light on specific parts of the photo resist. The resist is usually hard-baked before subjecting to a chemical etching stage which will remove the metal underneath. Finally, the hardened photo resist is etched using a different chemical treatment, and all that remains is a layer of metal in the same shape as the mask. The lithography process is used because it gives exact control over the shape and size of the objects it creates, and because it can create

¹⁶ Google, <http://images.google.com/imgres?imgurl=http://www.alacritas-consulting.com>. (November 2006).

patterns over an entire surface at the same time. The diagram below shows a picture of the spinner used to apply the photo resist. Specifics concerning the lithography are (for example):

- Alignment tolerance: $100\mu m$
- Alignment type: flat
- Wafer diameters: 50mm, 75mm, 100mm, and 150mm
- Resist thickness: 10mm



Figure 14. A spinner used to apply photo resist to the surface of a silicon wafer¹⁷

Finally, the process includes electroplating (see Figure 15). This is the coating of an electrically conductive item with a layer of metal using electrical current. The result is a thin, smooth, coat of metal on the object. The process used in electroplating is called electro deposition. The item to be coated is placed into a container containing a solution of a few metal salts. The item is connected to an electrical circuit, forming the cathode (or negative end) of the circuit while an electrode typically of the same metal to be plated forms the anode (or positive end). When an electrical current is passed through the

¹⁷ Answers Corporation: Online Encyclopedia, www.answers.com. (December 2006).

circuit, ions in the solution are attracted to the item. The result is a thin layer of metal on the item. The diagram below shows this process. Electroplating specifics are (for example):

- Temp: 20°C
- Thickness: $100\mu\text{m}$
- Material: copper
- They intend on electroplating both sides of the substrates

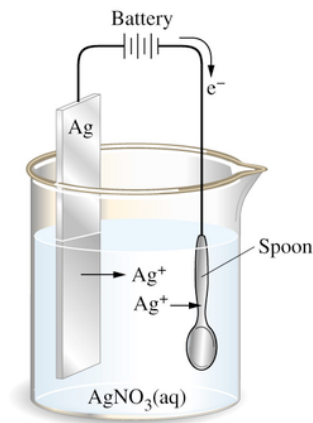


Figure 15. Electroplating process: For this diagram the anode is a silver bar and the cathode is an iron spoon¹⁸

2. Actual Wafers

The process above may also include using ultrasonic micromachining to etch out the glass holes. As can be seen, the fabrication process is very detailed and requires much equipment and time which can be very expensive to have it done depending on the type of material one wants to use. Currently, the idea is to continue using copper and glass as our substrate.

It was found that developing this microsystem in L-Edit and having it manufactured would cost \$17,000.00. Therefore, a more practical route had to be taken.

¹⁸ Google,
<http://images.google.com/images?svnum=10&hl=en&lr=&q=electroplating+process&btnG=Search>.
(December 2006).

We found a cost effective method by ordering Copper Clad FR-4-1/2 Oz. double side sheets 0.005”x 36” x 48” from JJ Orly¹⁹. Specifically, the G10-FR4 Cooper Clad is a fire rated electrical-grade, dielectric fiberglass laminate epoxy resin system combined with glass fabric substrate laminated to copper. The measurements are given in Table 1 below. As stated earlier, the Cooper Clad came in large sheets that first had to be cut into 2”x 2” samples, then precision drilled according to specifications as detailed in section.

C. EQUIPMENT DESCRIPTION

The equipment used for the experiments was essential for gathering and recording the data needed to produce the Paschen curves. Below are short descriptions along with photos. Together they should aid in understanding how the experiments were performed and data was recorded. A Mitutoyo micrometer was used for measuring the thickness of the samples. It recorded the thickness in inches as well as millimeters. Table 1 shows the data collect for our experimental wafers. The Table displays Thick, Middle, and Thin. This can also be referred to as A, B, and C respectively. The photos below show samples before the experiments where performed (See Figures 16-18).

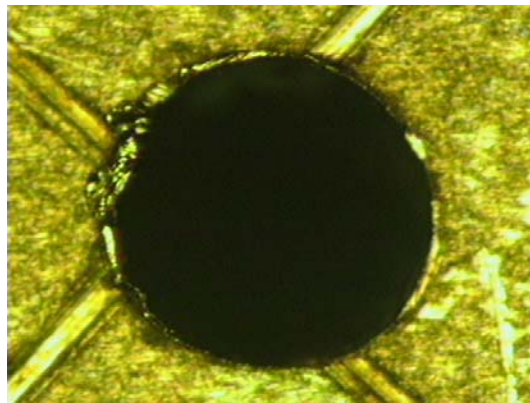


Figure 16. 300 μm sample diameter hole in $\text{Cu} - \text{Si}_2\text{O}_3 - \text{Cu}$ structure (Microscope Facility-courtesy of Prof. McNelley)

¹⁹ JJ Orly Inc., http://www.jjorly.com/g10_fr4_sheets_fabricator.htm. (November 2006).

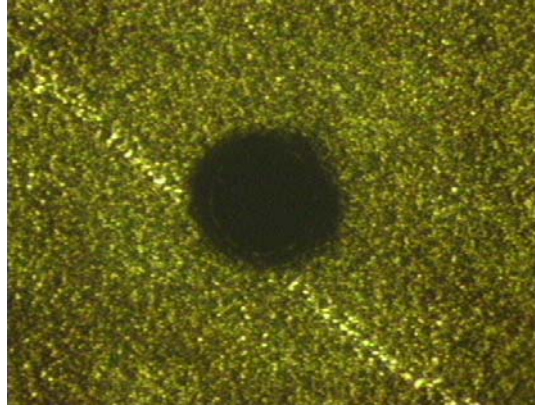


Figure 17. 400 μm sample diameter hole in $\text{Cu} - \text{Si}_2\text{O}_3 - \text{Cu}$ structure (Microscope Facility-courtesy of Prof. McNelley)

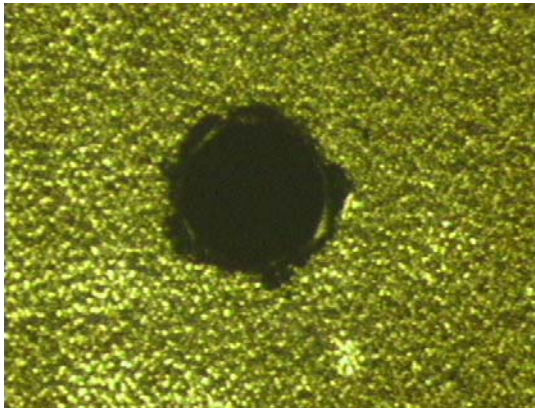


Figure 18. 500 μm sample diameter hole in $\text{Cu} - \text{Si}_2\text{O}_3 - \text{Cu}$ structure (Microscope Facility-courtesy of Prof. McNelley)

SAMPLE TYPE	Millimeters (mm)
Thick-No Holes	0.366
Middle-No Holes	0.287
Thin-No Holes	0.154
Thick-300 μm	0.372
Middle-300 μm	0.26
Thin-300 μm	0.136
Thick-400 μm	0.285
Middle-400 μm	0.284
Thin-400 μm	0.153
Thick-500 μm	0.384
Middle-500 μm	0.303
Thin-500 μm	0.137

Table 1. Chart of various thicknesses of samples used

Table 1 is a chart of the various thickness of the Cu electrodes and the dielectric. The electrical power supplied may produce in excess of 500 Volts. Due to safety, the power for the experiments was limited to 400 volts. If a breakdown voltage was not obtained at the 400 Volt limit, then the power was turned off and we recorded a no breakdown for the sample at that pressure. Figure 19 shows the power source used for out experiments. The power source, Kepco Labs 500R-B Power Supply Voltage, although much older, was reliable and lasted for the duration of the tests.



Figure 19. Kepco Labs 500R-B Power Supply Voltage

Making sure the pressure in the chamber was regulated correctly was very important for the experiments. This was done by reading the digital output of two sources. The one that was used, shown in Figure 20, was used once the chamber was at a pressure of below 75 Torr and the other shown in Figure 21. Before the chamber reached 75 Torrs of pressure, the Teranova Model 505A was used. After the 75 Torr was achieved the Varian 880RS Vacuum Ionization Gauge was used because it became more accurate at lower pressures. Both gages where helpful at different times while bringing up and down the pressure in the chamber.

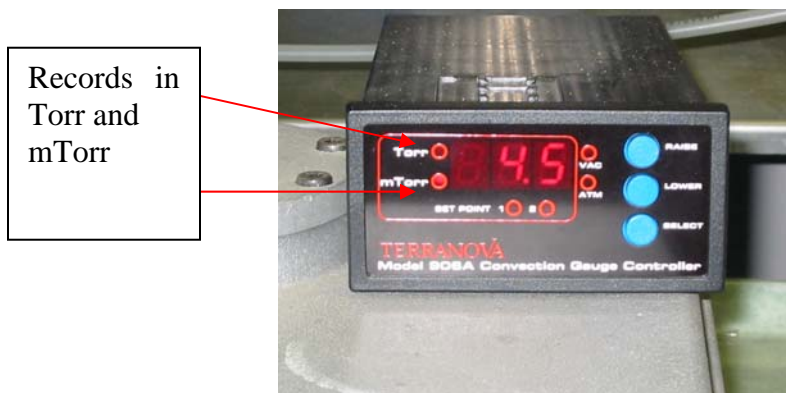


Figure 20. Terranova Model 505A Digital Pressure Recorder



Figure 21. Varian 880RS Vacuum Ionization Gauge

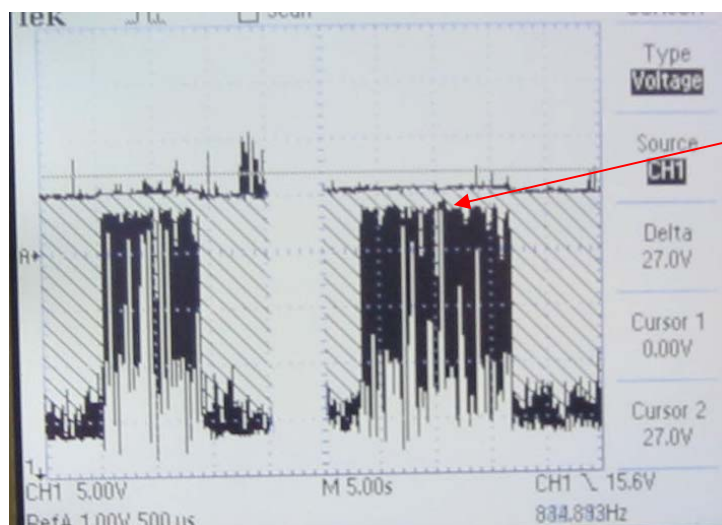
The voltage and amps were recorded using the Hewlett Packard 3478A Digital Multimeter. This multimeter has two separate boxes that measured each separately. We were only concerned with the readings for the amps. The voltage was recorded in two places. One being on the Tektronix TDS 1012 Two Channel Digital Storage Oscilloscope (see Figure 23 or Figure 24). This was the preferred place because the voltage supply operator could glance at the voltage shortly after breakdown voltage occurred. The other operator could concentrate on recording the amps from the Hewlett Packard 3478A Digital Multimeter when the other member informed the other when breakdown occurred.



Figure 22. The voltmeter (left) and amp meter (right) used for the experiments



Figure 23. Jason Cooper recording the breakdown voltage on a sample



Breakdown!

Figure 24. A close-up of the breakdown voltage occurring on the Tektronix TDS 1012

In order to pump the vacuum chamber down to the pressures needed to perform the experiments we used three different pumps: a turbo pump and two roughing pumps (see Figures 25 and 26). The Varian Turbo-V1000 was the workhorse pump. This pump was used when the vacuum chamber needs to be pumped to very low pressures. In order

to reduce the load on this pump, the roughing pumps are used while the Varian Turbo-V1000 is isolated via the isolated valve. The Varian SD-450 and Edwards roughing pumps were used for different purposes. The Varian SD-450 (see Figure 26) is the roughing pump while the Edwards (Figure 26) is used to vary the pressures during the experiment.

For example, after a particular experiment had been performed, the chamber was brought down to lower pressures before refilling. To do this the Varian Turbo-V1000 was isolated via the isolation valve and the Varian SD-450 was turned on until the pressure was brought down to about 75 Torr. At this time, the isolation valve was opened allowing the Varian Turbo-V1000 to bring the pressure down further so that experiments could be performed at various pressures to produce the Paschen curves.

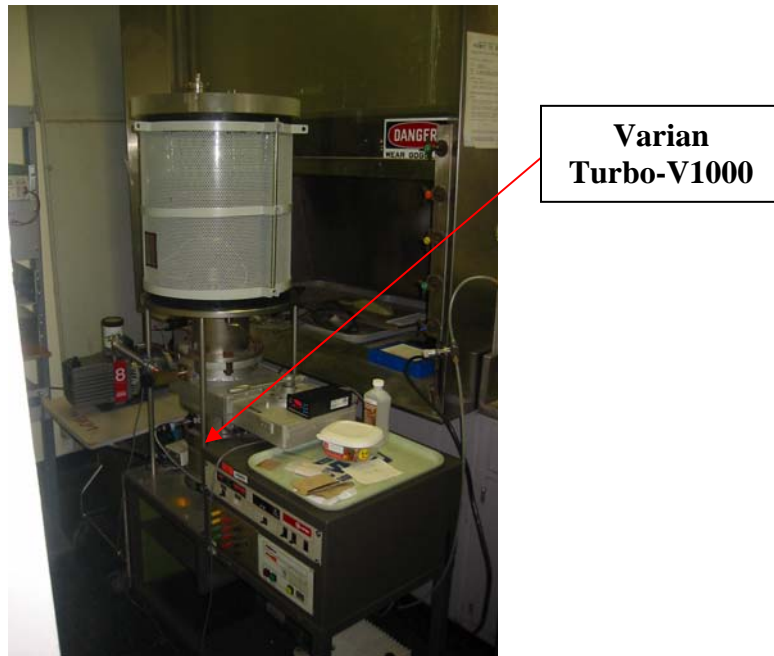


Figure 25. System set-up displaying the Varian Turbo-V1000



Figure 26. Varian SD-450 (left) and Edwards roughing pump (right)

The Paschen curves could not have been produced unless the pressure, voltages, and gas mixtures were precise. In order to precisely meter the Argon gas used for the experiments a fine metering valve was used (see Figure 27) while the pressure was watched closely. The pressure gauge on the Argon bottle was only used to make sure there was plenty of Argon needed to perform the experiments. Altogether, very little Argon was needed for these experiments. The Argon bottle was primarily a means of hooking up a connection to the chamber so that Argon gas could be metered into the vacuum chamber at various pressures. First, the bottle gauges were checked for ample amount. Next, the connection to the vacuum chamber was checked. Once the Argon was ready to be released, the precise metering pin was used to allow small and large amounts of Argon into the tank until the desired pressure was achieved. The pressures were able to be met very precisely at higher pressures and were difficult to achieve at lower pressures. There was evidence of a small leak-thus making it difficult to operate at very low pressures.



Figure 27. Precise metering value



Figure 28. Argon bottles next to vacuum chamber set-up

Finally, without good samples, it would have been impossible to obtain proper data. As stated earlier, $300\ \mu\text{m}$, $400\ \mu\text{m}$, and $500\ \mu\text{m}$ diameter holes were drilled (see

Figure 29). Figure 30 is the microscope used in obtaining Figures 16-18. The need to etch all samples was necessary as well to force the breakdown to occur around the holes (see Figure 31).

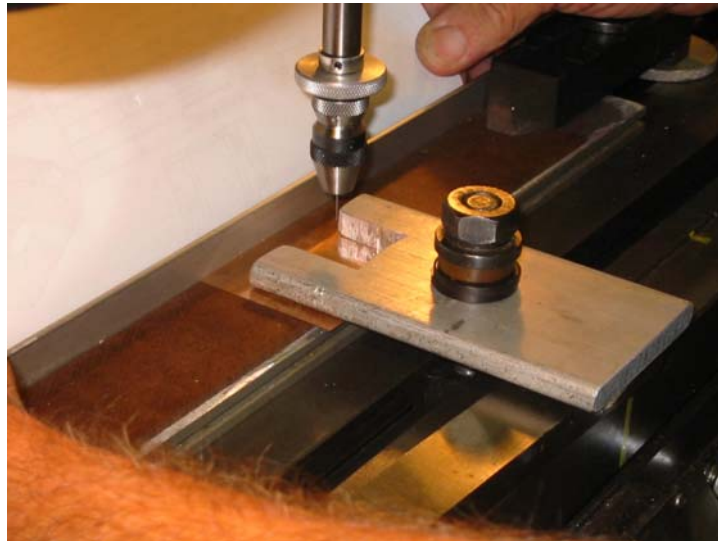


Figure 29. Precision Drill Press used to create the micron holes



Figure 30. Optical Microscope used to measure the MSE



Figure 31. Etching tank

The fabrication of the pre-manufactured wafers was tedious yet effective. The Paschen cures were simulated and we were able to focus the breakdown voltage around the holes which was the ultimate goal. This proved to be a cost effective alternate method of achieve desired results. Future work will consider the purchase of professionally manufactured microstructures, which should produce more precise results.

V. CONCLUSIONS AND RECOMMENDATIONS

A. SUMMARY

It has been shown that the fabrication of an ideal micro ionizer by using MEMS processes is ideal." This is most desirable and would be the most accurate situation for this project. However, due to financial constraints, using the Cu-glass-Cu laminated structures proved to be more practical. These served their purpose in that they allow for a reliable way to test our configurations of obtain Paschen curves (see Appendix C, Figures 32-34). Generating the Paschen curves using various samples under various pressures was the primary goal of this thesis, in Appendix C.

The Paschen curves showed three curves produced on three different graphs for the thick, middle, and thin samples for each hole diameter. Graph 1 displays this data for the 300 μm sample. The thick Paschen curve, in black, had the lowest breakdown voltage. The Graph also shows that it had the largest pd between plates. This discrepancy between thickness and voltage was consistent for all three graphs. The one constant observation was the relationship between "pd" and thickness. The thin wafers, regardless of hole size, consistently had the lowest pd followed by the middle, and thick wafers respectively. This confirms the data obtained during the experiments²⁰. The thinner Cu-glass-Cu structures, the lower the breakdown voltage.

B. RECOMMENDATIONS FOR FUTURE WORK

A very good basis for ongoing future experiments has been established. Several suggestions can be made to make the set-up better and more efficient. Currently, the process for performing the experiments is a two man job. One person must be record data and be a coordinator while the other is running up the voltage and making the appropriate calls when breakdown occurs so that the amps can be recorded at the right time. A computer with an interface card could record all data being taken including amps, breakdown voltage, and the pressure. This may reduce the process for performing the experiment to a one-person job. There is also a possibility manufacturing of a smaller vacuum chamber. This could require a much shorter time to pump down the chamber to the desired pressure to perform the experiments. Additionally, a device could be

²⁰ Jason Cooper-Thesis Research, "Study of a Novel Ionization Chamber for Ion Thrusters."

designed to force the Argon gas into the center of the wafer where the holes are located. This would increase the chances that the breakdown will be localized around the holes rather than the edges and chamber.

In the future, a custom microsystem could be fabricated using a design from the L-Edit program. After the microsystems have been designed, funding will hopefully be obtained and a microsystem will be purchased. This should produce much cleaner Paschen curves due to the more precise etching process rather than holes that have been drilled into a pre-constructed wafer.

APPENDIX A. GLOSSARY OF TERMINOLOGY

Ag	SILVER
AgNO	SILVER NITRATE
Ar	ARGON
DC	DIRECT CURRENT
FEEP	FIELD EMISSION ELECTRIC PROPULSION
G10FR4	EPOXY GLASS CLOTH LAMINATE SHEET
LT	LIEUTENANT
MEMS	MICROELECTROMECHANICAL SYSTEMS
MSE	MICRO-STRUCTURED ELECTRODE
TC	THERMO COUPLES
TDS	TEKTRONIX DIGITAL STORAGE
TORR	Millimeter of Hg [13, 33 N/ m^2]
NASA	NATIONAL AERONAUTICS AND SPACE ADMINISTRATION
pd	PRESSURE x ELECTRODE SEPARATION DISTANCE
ln	NATURAL LOGARITHMS
μm	MICROMETERS
γ	GREEK LETTER GAMMA (SECONDARY SURFACE ELECTRON EMISSION)

THIS PAGE INTENTIONALLY LEFT BLANK

APPENDIX B. MATLAB CODE FOR GRAPHS

```
clear all

close all

clc

d1=.0137; %cm or 0.00535in

P1=[35.2 51.3 82.2 103 151 202 509]; %% pressure in millitorr

P1=P1/1000; %% pressure in torr

Vb1=[326 292 262 244 252 260 302]; %% voltage in volts

pd1=d1*P1;

d2=.0303; %cm or 0.0119in

P2=[33.9 50.9 80.7 106 159 208 503]; %% pressure in millitorr

P2=P2/1000; %% pressure in torr

Vb2=[296 276 248 258 258 274 324]; %% voltage in volts

pd2=d2*P2;

d3=.0384; %cm or 0.0151in

P3=[32.2 50.7 84.1 100 149 200 518]; %% pressure in millitorr

P3=P3/1000; %% pressure in torr

Vb3=[382 320 284 234 262 276 348]; %% voltage in volts

pd3=d3*P3;

figure(1)

plot(pd1,Vb1,'bo-','linewidth',2)

hold on

plot(pd2,Vb2,'rs:','linewidth',2)

hold on
```

```

plot(pd3,Vb3,'k^--','linewidth',2)

hold on

grid on

title('Paschen curves of wafers with 300um diameter holes.')

xlabel('pd (torr-cm)')

ylabel('Vb (Volts)')

legend('Thin','Middle','Thick','Location','SouthEast')

d1=.0153; %cm or 0.00605in

P1=[32.1 52.9 82.9 98.3 154 204 517]; %% pressure in millitorr

P1=P1/1000; %% pressute in torr

Vb1=[364 310 276 264 254 276 348]; %% voltage in volts

pd1=d1*P1;

d2=.0284; %cm or 0.01115in

P2=[31.8 48 84.3 107 152 200 500]; %% pressure in millitorr

P2=P2/1000; %% pressute in torr

Vb2=[332 318 284 280 284 298 360]; %% voltage in volts

pd2=d2*P2;

d3=.0285; %cm or 0.0112in

P3=[30.3 51.3 83.7 102 150 203 498]; %% pressure in millitorr

P3=P3/1000; %% pressute in torr

Vb3=[326 310 290 270 282 334 354]; %% voltage in volts

pd3=d3*P3;

figure(2)

plot(pd1,Vb1,'bo-','linewidth',2)

```

```

hold on

plot(pd2,Vb2,'rs:', 'linewidth',2)

hold on

plot(pd3,Vb3,'k^--', 'linewidth',2)

hold on

grid on

title('Paschen curves of wafers with 400um diameter holes.')

xlabel('pd (torr-cm)')

ylabel('Vb (Volts)')

legend('Thin','Middle','Thick','Location','SouthEast')

d1=.0153; %cm or 0.00605in

P1=[35.1 50 83.8 102 148 199 500]; %% pressure in millitorr

P1=P1/1000; %% pressute in torr

Vb1=[316 284 266 256 264 326 364]; %% voltage in volts

pd1=d1*P1;

d2=.026; %cm or 0.01025in

P2=[31.7 56.6 81.4 101 150 200 499 800]; %% pressure in millitorr

P2=P2/1000; %% pressute in torr

Vb2=[322 290 260 250 272 318 300 340]; %% voltage in volts

pd2=d2*P2;

d3=.0372; %cm or 0.01465in

P3=[30.7 50.6 83.1 98.2 149 198 498]; %% pressure in millitorr

P3=P3/1000; %% pressute in torr

Vb3=[346 346 308 298 298 282 352]; %% voltage in volts

```

```

pd3=d3*P3;
figure(3)
plot(pd1,Vb1,'bo-', 'linewidth',2)
hold on
plot(pd2,Vb2,'rs:', 'linewidth',2)
hold on
plot(pd3,Vb3,'k^--', 'linewidth',2)
hold on
grid on
title('Paschen curves of wafers with 500um diameter holes.')
xlabel('pd (torr-cm)')
ylabel('Vb (Volts)')
legend('Thin','Middle','Thick','Location','SouthEast')

```

APPENDIX C. GRAPHS OF SAMPLES BY HOLE SIZE

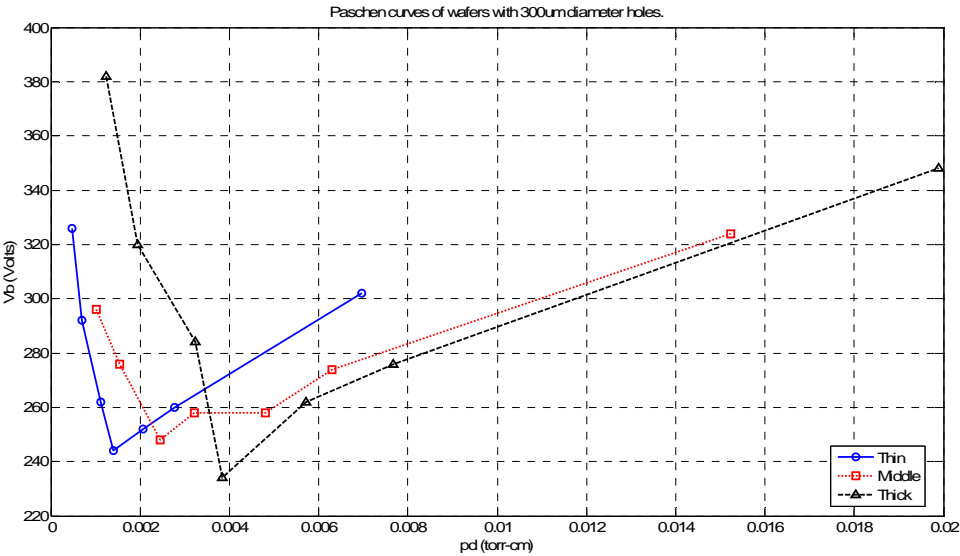


Figure 32. Experimental Results (Paschen Curves) (300 μm)

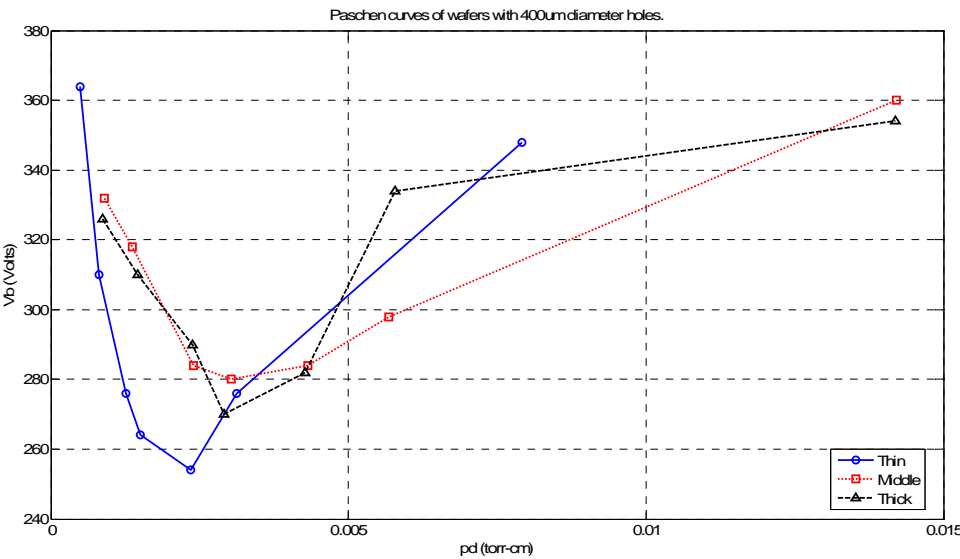


Figure 33. Experimental Results (Paschen Curves) (400 μm)

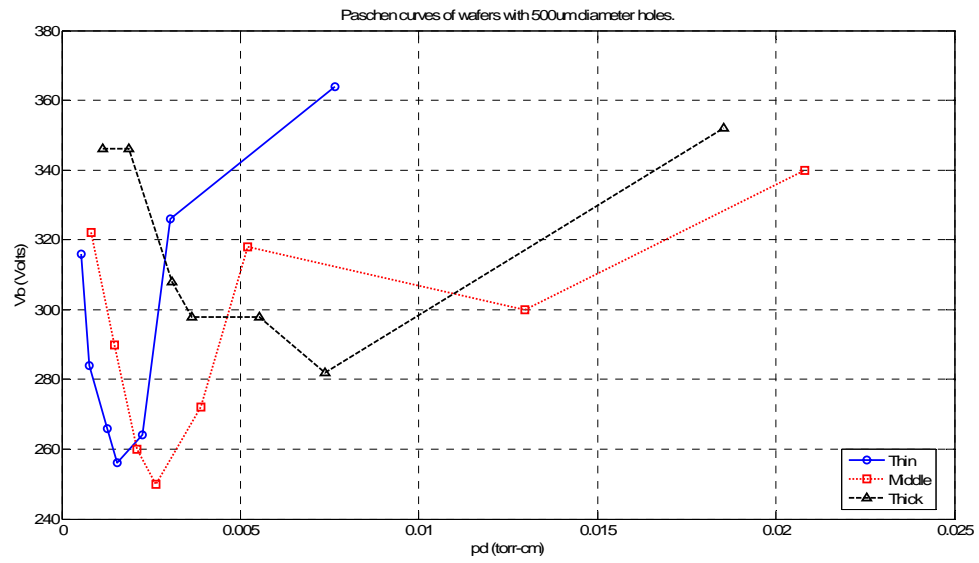


Figure 34. Experimental Results (Paschen Curves) ($500\ \mu m$)

APPENDIX D. VACUUM SET-UP DIAGRAMS

A. THIS SECTION WILL COVER THE PROCEDURE FOR VACUUM CHAMBER OPERATION

Steps:

Vent vacuum chamber to normal atmospheric pressure by opening venting valve.

Open vacuum chamber and connect wafer to copper leads utilizing plastic clips. Ensure that the two copper leads are attached on opposite sides of the wafer from each other.

Close vacuum chamber and inspect seals. Ensure venting valve and roughing pump number 2 valve are closed. Open isolation valve and start roughing pump number 1.

Turn on instrument panel and thermocouple (TC) gages 1 and 2 and 3. Once TC2 and TC3 indicate chamber pressure around 100 millitorr turn power on to the Turbo Molecular Pump (TMP) and monitor as power up sequence commences. Turn on Filament gage and monitor pressure.

Once vacuum chamber pressure is at its minimum pressure (approximately 1.5×10^{-6} torr) fasten Argon line to vent valve on chamber and ensure metering valve is closed (see Figure 36). Open pressure valve on Argon tank and open cut off valve to metering valve on argon line to vacuum chamber (see Figure 37).

Close Isolation Valve and begin backfilling vacuum chamber with Argon by opening vent valve and open metering valve. Adjust and control flow of Argon into Vacuum chamber by adjusting metering valve and monitoring TC3 meter (see Figure 35 below).

Once pressure in vacuum chamber has reached required pressure shut off metering valve and close vent valve.

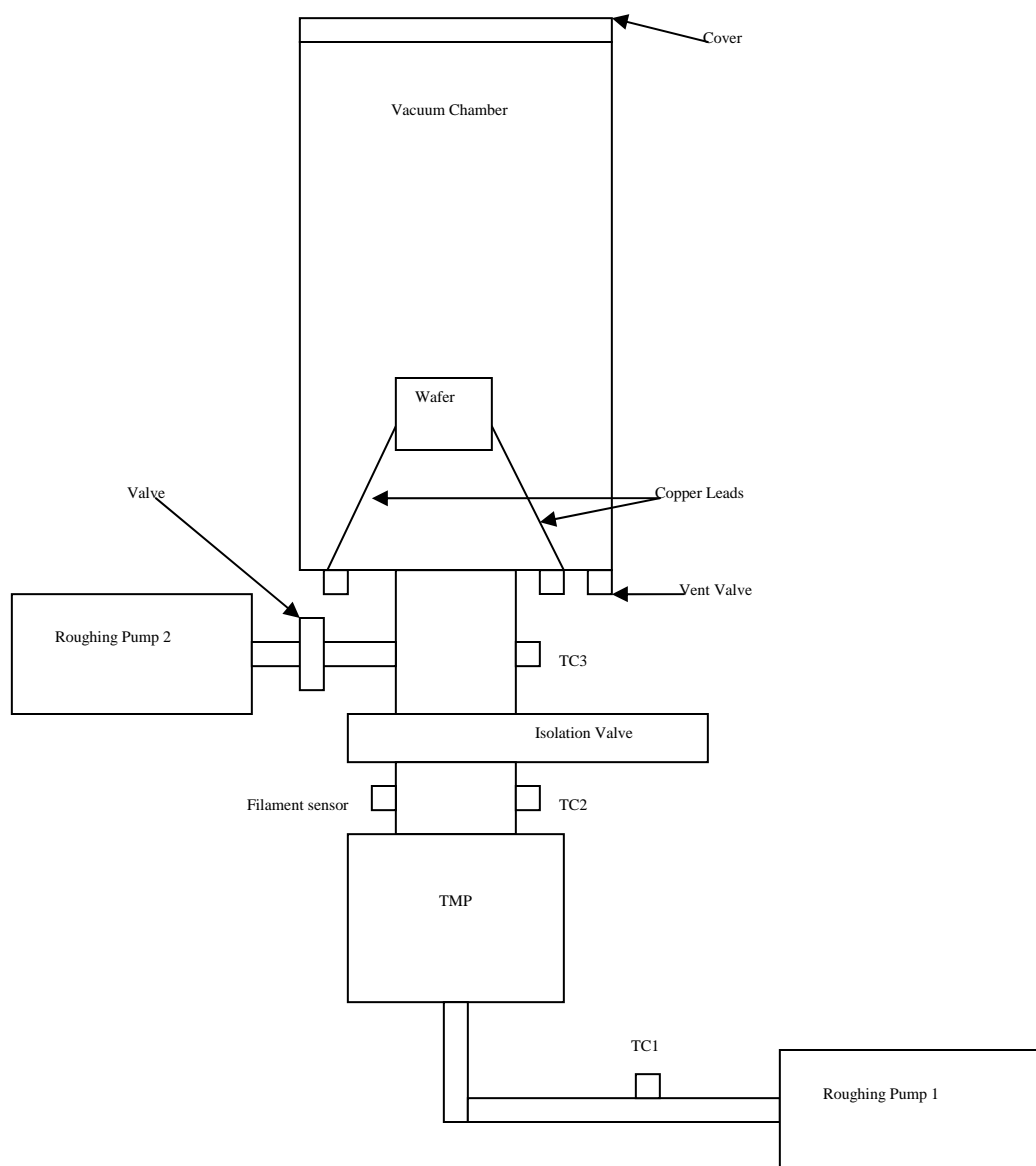


Figure 35. Schematic drawing of vacuum set-up

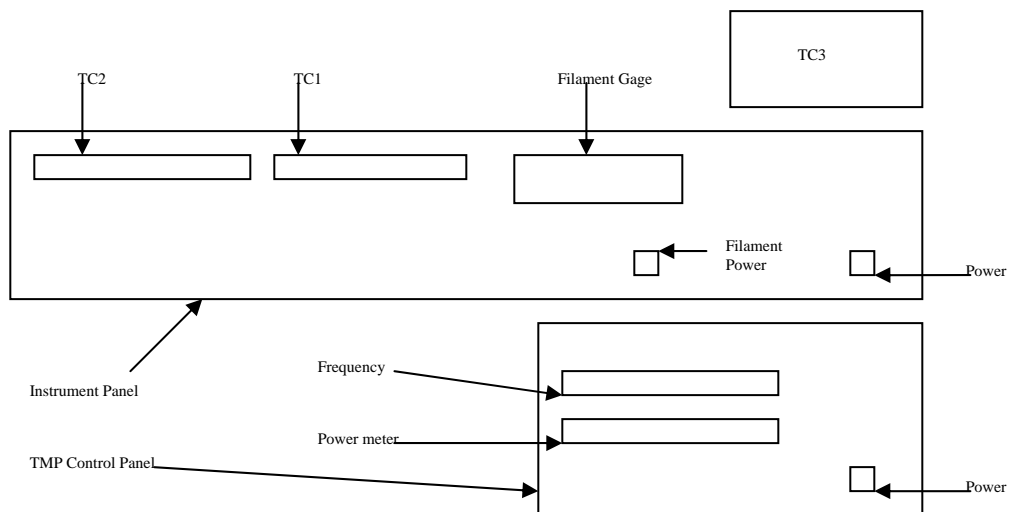


Figure 36. Schematic drawing of Varian 880RS Vacuum Ionization Gauge

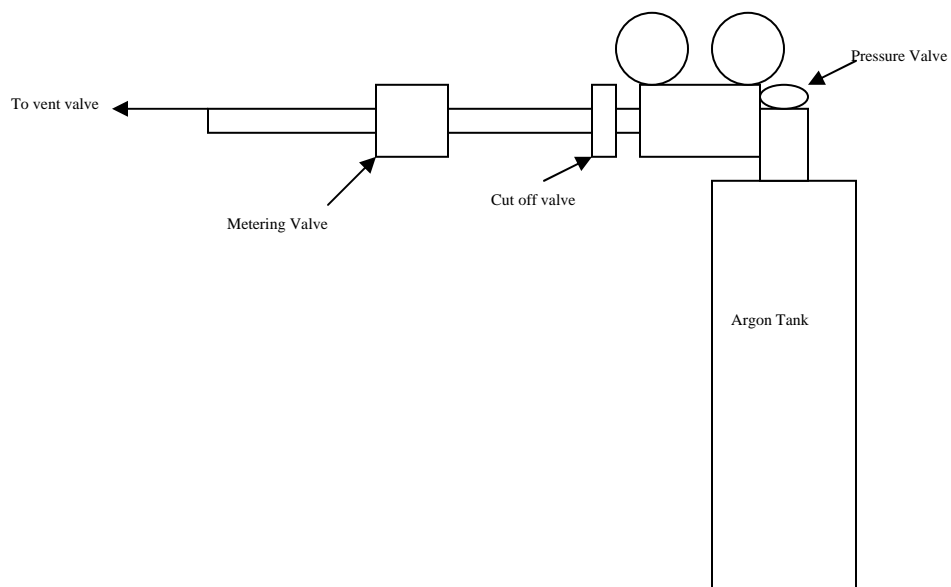


Figure 37. Schematic of Argon bottle, gauge, and valves used for metering

B. THIS SECTION WILL COVER THE PROCEDURE FOR INSTRUMENT PANEL OPERATION

Steps:

Once the procedures in part A is complete and the experiment is ready to be run, turn on power to the equipment cabinet ensuring that the voltmeter, amp meter and oscilloscope power up.

Switch amp meter from AC to DC setting. Voltmeter should default to DC setting. Set oscilloscope to 5 volts per division and 5 seconds per division (see Figure 38).

For Safety Ensure No One is touching any wires or the vacuum chamber.

Ensure power supply is set to zero volts and turn on power supply.

Begin by incrementing voltage levels and monitor oscilloscope and voltmeter for breakdown voltage.

Once breakdown voltage has been achieved record voltage and turn off power supply and set dials on power supply back to zero volts.

Set up for next experiment.

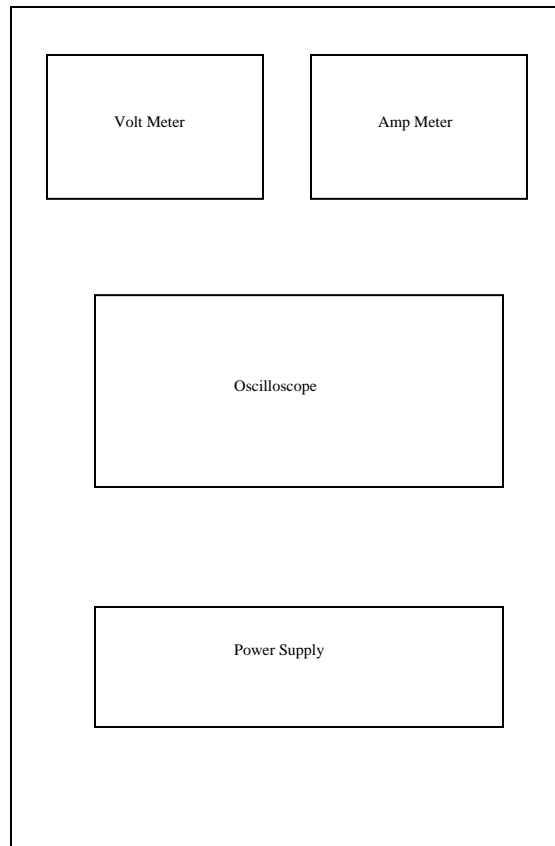


Figure 38. Schematic drawing of Electrical Rack

THIS PAGE INTENTIONALLY LEFT BLANK

LIST OF REFERENCES

- Biblarz .O. and Sinibaldi, J., “Study of DC Ion Thrusters with Argon Propellants,” Abstract submitted to the AIAA-JPC, Sacramento, CA, 2006.
- Biblarz, O. and Bell, W. J., “Thermionic Arc Breakdown in Small Discharge Gaps: Model and Application,” IEEE Transactions on Industry Applications, Vol. 34, No. 2, March/April 1998, pp. 325-331.
- Boeing, <http://www.boeing.com>, November 25, 2006.
- Cooper, Jason, Thesis Research, “Study of a Novel Ionization Chamber for Ion Thrusters,” Master’s Thesis, Naval Postgraduate School, December 2006.
- Google, <http://images.google.com>, November 25, 2006.
- Humble. Ronald W., Henry, Gary N. and Larson, Wiley J., “Space Propulsion Analysis and Design,” 1995 by the McGraw-Hill Companies.
- JJ Orly, http://www.jjorly.com/g10_fr4_sheets_fabricator.htm, November 25, 2006.
- John Glenn Research Center, National Aeronautics and Space Administration, <http://www.grc.nasa.gov/WWW/ion/overview/overview.htm>, November 25, 2006.
- L-Edit Design Tool.
- Nasser, E., *Fundamentals of Gaseous Ionization and Plasma Electronics*, John Wiley & Sons, Inc., 1971.
- Parallel Synthesis Technologies, www.parallelsynthesis.com, November 25, 2006.
- Penache, M. C., “Study of High Pressure Glow Discharges Generated by Micro-Structured Electrode (MSE) Arrays,” PhD Dissertation, Frankfurt am Main University, Germany, 2002.
- PH3280-MEMS Design I Class.
- Science@NASA, http://science.nasa.gov/newhome/headlines/prop06apr99_2.htm, November 25, 2006.
- Senturia, Stephen D. “Microsystem Design,” Springer Science+Business Media, Inc., 2001.
- Sinibaldi, J. and Biblarz, O., “Thermionic Ion Propulsion (TIP) Concept,” Proposal submitted to DARPA, 2003.

Sutton, G. P. and Biblarz, O., "Rocket Propulsion Elements," VIIth Edition, Wiley, NY, 2001.

Wikipedia, The Free Encyclopedia, http://en.wikipedia.org/wiki/Ion_engines, November 25, 2006.

INITIAL DISTRIBUTION LIST

1. Defense Technical Information Center
Ft. Belvoir, Virginia
2. Dudley Knox Library
Naval Postgraduate School
Monterey, California
3. Head, Information Operations and Space Integration Branch, PLI/PP&O/HQMC,
Washington, DC
4. Professor Jose O. Sinibaldi
Department of Mechanical and Astronautical Engineering
Naval Postgraduate School
Monterey, California
5. Professor Oscar Biblarz
Department of Mechanical and Astronautical Engineering
Naval Postgraduate School
Monterey, California